Journal of Architectural Research and Development, 2024, Volume 8, Issue 2
http://ojs.bbwpublisher.com/index.php/JARD
Online ISSN: 2208-3537
Print ISSN: 2208-3529

# Analysis and Comparison of Slope-cutting Widening Schemes in Highway Reconstruction and Expansion Project Based on MIDAS Software

**Zhiqiang Qiu*, Yun Shi, Lei Jiang**

China Merchants Chongqing Communications Technology Research & Design Institute Co., Ltd., Chongqing 400067, China

***Corresponding author:*** Zhiqiang Qiu, qiuzhiqiang1@cmhk.com



**Abstract:** In this paper, the geological condition of the right-side slope of the K114 + 694–K115 + 162 section of Yong-tai-wen Expressway is investigated and analyzed with the results showing that the strength of rock mass is the main contributor to the stability of the slope. Then, two widening schemes are proposed, which are the steep slope with strong support and the gentle slope with general support schemes. The static/slope module of MIDAS GTS finite element analysis software and the strength reduction method were used to compare the two schemes. The results show that the steep slope with a strong support scheme has obvious advantages in land requisition, environmental protection, and safety and is more suitable for reconstructing and expanding the highway slope.

**Keywords:** Highway reconstruction and expansion; Slope excavation; MIDAS GTS; Scheme selection

**Online publication:** March 27, 2024

## 1. Introduction

As the happiness index of people living in China increases daily, road traffic volume also increases proportionally. Existing highways can no longer meet the travel requirements of the people. Traffic jams and accidents frequently occur on many roads in various regions, especially during holidays. This phenomenon negatively impacts the lives of people, so it is particularly important to resolve traffic bottlenecks and smoothen traffic. Many areas tend to reconstruct and expand existing highways since building new highways requires large investments and land occupation. However, excavation on the existing road will inevitably affect the stability of the original slope. In addition, the reconstruction and expansion of the road may pose a certain safety threat to passing vehicles. Therefore, choosing a reasonable, safe, and effective existing slope widening and excavation scheme is particularly critical.

Domestic and foreign scholars have studied the slope widening scheme in highway reconstruction and expansion projects. Chen analyzed the stability and instability characteristics of the expansion soil slope excavation and proposed an approach to slope treatment for reconstruction and expansion that involves pre-reinforcement, support strengthening, and minimal excavation [1]. Lin used $FLAC^{3D}$ software to simulate two slope-widening construction schemes: stepped cross-section excavation and anti-slide pile + anchor cable pre-reinforcement excavation, and concluded that the latter technique has a more obvious reinforcement effect on slopes and is more suitable for slopes with complex surrounding environments [2]. Zhou simulated the entire process of highway reconstruction and expansion slope engineering, analyzed the plastic strain of the slope-cutting excavation and displacement field distribution, and evaluated the overall stability of the slope [3]. Chen summarized and studied the key points of safety protection technology for high slope-cutting construction in highway reconstruction and expansion based on different natural resource conditions [4]. Sun compared the slope widening methods of highway reconstruction and expansion, pre-reinforcement, and post-excavation, and concluded that pre-reinforcement of the existing slope before excavation would greatly improve its reliability [5]. He simulated and analyzed the slope-cutting construction scheme for highway reconstruction and expansion based on FLAC$^{3D}$ software [6]. Lu researched the secondary excavation of existing anchor rock slopes during the highway reconstruction and expansion process and concluded that the residual anchors play a positive role that cannot be ignored in the entire project construction process, so the utilization of existing supporting structures can be considered in subsequent similar reconstruction and expansion projects [7]. Gao conducted a stability analysis on the secondary excavation sequence of typical rocky high slopes in the reconstruction and expansion section and concluded that the combination of the original support and the new support can maximize the anti-slip protection effect and rationally utilize the original structure, improving the overall stability during slope excavation [8]. Feng analyzed the stability of the secondary excavation of the existing high slope of the widened expressway and concluded that the main failure factor of the secondary excavation slope is cracks from slip tension [9]. Zhang conducted a series of analyses and comparisons on the excavation technology of rock slopes under the conditions of ensuring traffic flow and concluded that the excavation methods for slope reconstruction and expansion under different working conditions have certain significant impacts on similar projects [10].

Domestic research mostly uses FLAC$^{3D}$ software for simulation analysis of different scenarios while other geotechnical numerical simulation software is less utilized [11-13]. Based on this, this article uses the strength reduction method of MIDAS GTS (GeoTehnical analysis System) finite element numerical analysis software to perform numerical simulation for different excavation and support schemes for reconstructing and expanding the slope on the right side of K114 + 694–K115 + 162 (design pile number) of Yong-tai-wen Expressway, combined with economic, technical, safety, and other indicators for comprehensive comparison, to provide reference for similar projects.

## 2. Project overview

The current maximum slope height of the excavation site on the right side of K114 + 694–K115 + 162 of the Yong-tai-wen Expressway is about 44 m, totaling 6 levels. Each level of the first five slopes is 8 m high. The slope ratio is 1:0.25, 1:1.0, 1:1.0, 1:1.0, 1:1.0, 1:1.0 respectively. The overlying residual slope accumulates gravelly silty clay with a thin thickness of about 1.0 to 3.0 m, and the lithology of the slope is a strongly weathered layer of granite with a thickness of about 1.5 to 4.0 m. The weathered rock mass consisted of rocks that are relatively complete to relatively broken. The body joint fissures of the slop are relatively developed and locally dense. The main protection measures for the slope consisted of the first-level slope equipped with a sloping retaining wall built with mortar, while the second-level to sixth-level slopes are sprayed with grass. The main concerns are collapse and damage of the water intercepting ditch at the top of the slope, obvious deformation, and sliding marks on the top of the slope, with the current stability of the slope being average as shown in **Figure 1**.

The slope aspect is 86° ∠45°, and there are three main groups of joint fissures:

(1) 314° ∠76°, sparse, straight, and closed with a long extension.

(2) 175° ∠70°, 4–5 joints/m, straight closed extension length.

(3) 50° ∠75°, 3 to 4 pieces/m, straight closed extension length.

The red flat projection is shown in **Figure 2**.

**Figure 1.** A photo of the current slop

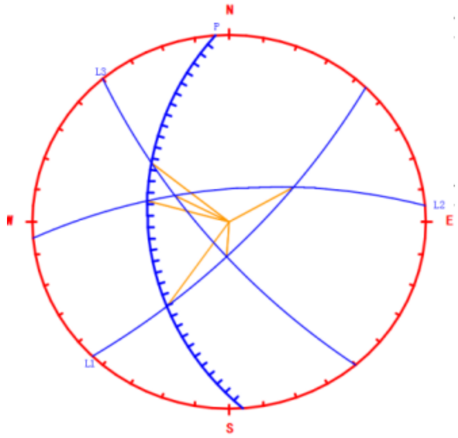


**Figure 2.** Stereographic projection map

According to the analysis of the stereographic projection map in **Figure 2**, it is shown that the three groups of cracks form an inverse slope or a tangential slope with the layer, which has little impact on the road. The intersection of each group of cracks is located outside the slope, which also has little impact on the stability of the slope. Therefore, the slope is stable mainly with the strength of the rock mass. The physical and mechanical parameters of the slope were determined based on experiments and local experience, as shown in **Table 1**.

**Table 1.** Mechanical parameters of slope

| Geotechnical category | Modulus of elasticity (Mpa) | Poisson's ratio | Natural state (joint surface) | | | Saturated state (joint surface) | | |
|---|---|---|---|---|---|---|---|---|
| | | | Bulk weight (kN/m) | Cohesion (kpa) | Friction angle (°) | Bulk weight (kN/m) | Cohesion (kpa) | Friction angle (°) |
| Gravelly silty clay | 30 | 0.36 | 19.5 | 60 | 18.0 | 20.5 | 54 | 16.3 |
| Strongly weathered granite | 10000 | 0.28 | 22.0 | 90 | 31.0 | 22.5 | 81 | 28.4 |
| Weathered granite | 16200 | 0.26 | 25.5 | 150 | 32.3 | 26.0 | 135 | 29.6 |
| Micro-weathered granite | 23200 | 0.24 | 27.0 | 200 | 38.0 | 27.5 | 180 | 35.1 |

Considering geological conditions, traffic protection scheme, environmental protection requirements, and project cost, the reconstruction and expansion of the slope cutting will consider and compare the following two schemes, steep slope foot with strong support and slow slope with general slope protection.

## 3. Computational model

### 3.1. Features of MIDAS GTS slope module

When MIDAS GTS finite element software solves the safety factor during slope stability analysis, it does not need to assume the shape and position of the slip surface as the software automatically calculates the slip surface.

The software can also output the settlement results of each step and analyze the slope damage process, allowing analysis of the stress, deformation, and stability coefficient of the current slope during the excavation and support process based on the principle of the strength reduction method.

The strength reduction method is also called the shear strength reduction method, the strength parameter reduction method, and so on. The basic principle is to gradually reduce the shear strength parameters of the soil until the soil slope topples. The multiple of the reduction, that is, the critical reduction coefficient, is defined as the safety factor. The basic formula is as follows:

$$c^{trial} = \frac{c}{F_{trial}}$$

$$\Phi^{trial} = arc\tan\left(\frac{\tan\Phi}{F_{trial}}\right)$$

Compared with the traditional limit equilibrium method, the shear strength reduction method has some outstanding advantages. For example, any sliding mode can occur naturally without presupposing the trial sliding surface, including the shape and position of the sliding surface. There is no need to make assumptions about the magnitude and direction of the forces between soil strips like the limit equilibrium method; at the same time, the soil-structure interaction can be fully considered, and the construction mechanical behavior of the project can be simulated [14,15].

## 3.2. Model establishment

A numerical model is established based on the actual engineering conditions. The first scheme is a steep slope foot with strong support that specifically adopts a two-level excavation. The cross-section height after excavation is 19.14 m. The slope ratio of the first-level slope is 1:0.3, and the excavation height of the second-level slope is 10 m. The slope ratio is 1:0.5, and a 2 m wide platform is set up between each level. After excavating the slope, the first and second levels are supported by 9 m-long anchor frame beams. The anchor spacing is 2 m, and the inclination angle is 15°. The second scheme is a gentle slope with general slope support with four excavation levels. The slope ratios from bottom to top are 1:0.5, 1:0.75, 1:1.00, and 1:1.25 respectively. The slope height of each level is 10 m. A 2 m wide platform is set up in the space. The slope height after excavation is 37.36 m. Active protection nets are used to protect the excavation slope. The distance between anchors is 2 m, and the inclination angle is 15°. The calculated mechanical parameters of the anchor are shown in the table below in **Table 2**. The excavation models are shown in **Figure 3–6** below respectively. The bottom boundary of the model is fixed, and the horizontal displacement is constrained laterally. The upper part is a free boundary, and the load is only gravity. The Moore-Coulomb criterion is used to describe the rock and soil mass.

**Table 2.** Mechanical parameters of anchor

| Project | Resilience model (GPA) | Cross-sectional area ($m^2$) | Poisson's ratio | Drilling diameter (mm) |
|---|---|---|---|---|
| Anchor rod | 10 | 0.0005 | 0.25 | 110 |

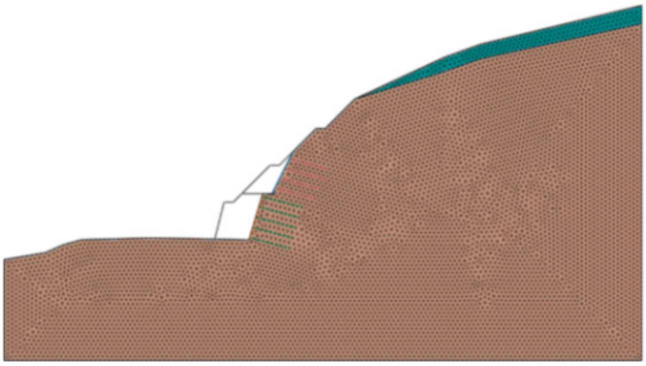

**Figure 3.** Excavation diagram of Scheme 1

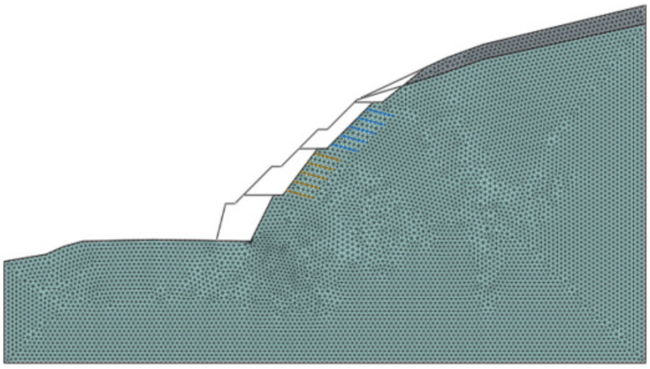

**Figure 4.** Excavation diagram of Scheme 2

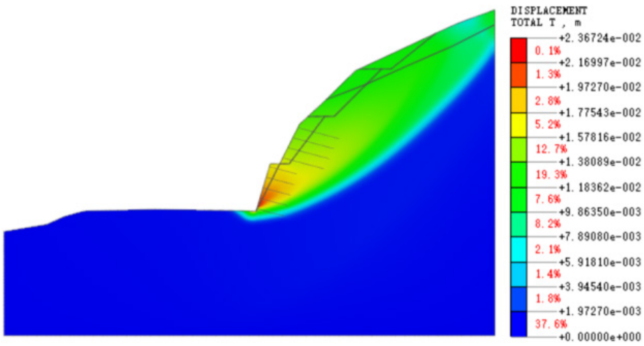


**Figure 5.** Total displacement nephogram with Scheme 1 excavation

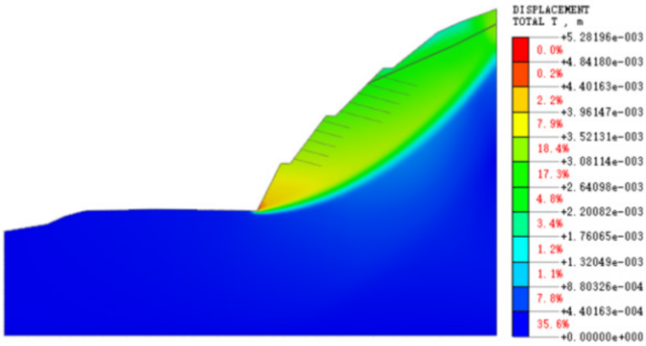


**Figure 6.** Total displacement nephogram with Scheme 2 excavation

## 4. Analysis of calculation results

For the steep slope with a strong support solution in Scheme 1, the steps for numerical simulation of slope support are as follows: Calculate the initial stress of the slope, excavate the first-level slope, excavate the second-level slope, determine the slope stability, and install slope support. Before excavation, the safety factor of the slope was 1.43, and the slope was stable. The rock and soil parameters obtained for side verification were relatively reasonable. After excavation, the safety factor of the slope was 1.28, which was lower than that mandated in the "Highway Subgrade Design Code," which listed that the safety factor under normal working conditions is >1.3, while the safety factor under abnormal working conditions is >1.2. After the first and second-level slopes are supported by 9 m long anchor rods, the safety factor of the slope is 1.36, which meets the specification requirements, indicating that the anchor support has achieved a certain effect.

**Figure 7** shows the final horizontal displacement deformation incremental cloud diagram after the slope excavation and support are completed. The horizontal displacement is in the shape of a sliding surface, with the maximum horizontal displacement being 5.2 cm and appearing near the foot of the slope, indicating that stress is concentrated at the foot of the slope which is more prone to instability than other locations.

**Figure 8** shows the final equivalent plastic strain cloud diagram after the slope excavation and support are completed. Similar to the horizontal displacement, the equivalent plastic strain also takes the shape of a sliding surface. The plastic strain at the top is not obvious, and the maximum strain value at the foot of the slope is 0.0174, showing that the foot of the slope is the most vulnerable to instability.

**Figure 9** shows the final maximum principal stress cloud diagram after the slope excavation and support are completed. It can be seen from the figure that the maximum principal stress on the slope surface is compressive stress, located near the top of the slope, with a maximum value of 100.97 kPa at the foot of the slope. The maximum principal stress is small, indicating the support has an effect.

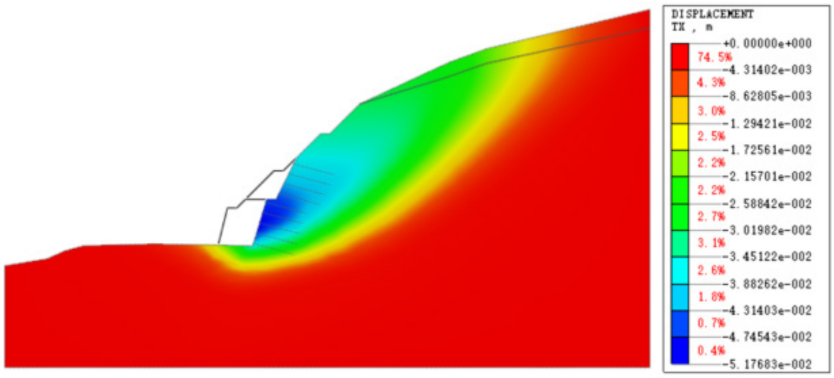


**Figure 7.** The horizontal displacement nephogram after excavation and support in Scheme 1

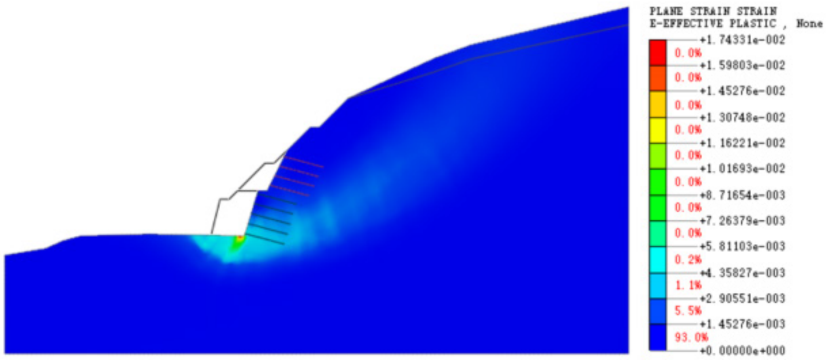


**Figure 8.** The effective plastic nephogram after excavation and support in Scheme 1

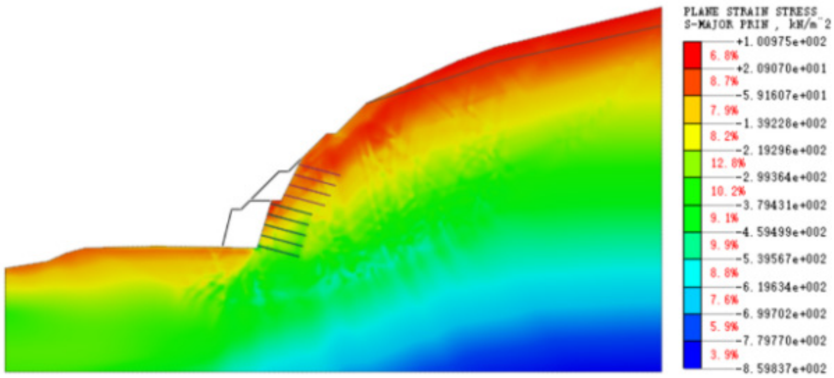


**Figure 9.** The maximum principal stress nephogram after excavation and support in Scheme 1

Scheme 2 consists of a gentle slope with general support. The steps for numerical simulation of slope support are to calculate the initial stress of the slope, excavate the first-level slope, excavate the second-level slope, excavate the third-level slope, excavate the fourth-grade slope, judge the slope stability, and install slope support. Similar to Scheme 1 before excavation, the safety factor of the slope is 1.43, and the slope is stable. After excavation, the safety factor of the slope is 1.31, which meets the specification requirements. Therefore, after excavation using this method, only the active slope surface of the protective net is used for general protection to prevent weathering and falling of blocks from the slope surface, which will affect the safety of drivers below.

**Figure 10** shows the final horizontal displacement deformation incremental cloud diagram after the completion of the excavation and support of the second slope of the scheme. The overall horizontal displacement is in the shape of a sliding surface. The maximum horizontal displacement is 3.5 cm and appears near the foot of the slope, indicating that stress is concentrated at the foot of the slope and is more prone to instability than other locations.

**Figure 11** shows the final equivalent plastic strain cloud diagram after the excavation and support of the second slope of the scheme are completed. Similar to the horizontal displacement, the equivalent plastic strain also takes the shape of a sliding surface. The plastic strain at the top is not obvious, and the maximum strain value at the foot of the slope is 0.0121, which also shows that the foot of the slope is the most vulnerable to instability.

**Figure 12** shows the final maximum principal stress cloud diagram after the slope excavation and support are completed. It can be seen from the figure that the maximum principal stress on the slope surface is compressive stress, located near the top of the slope, with a maximum value of 54.84 kPa.

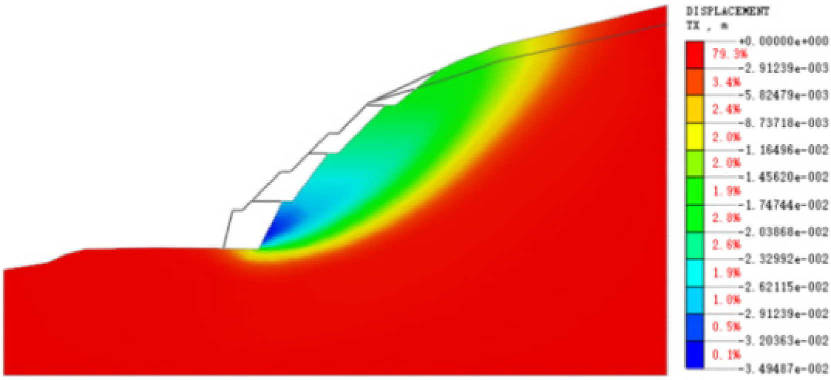


**Figure 10.** The horizontal displacement nephogram after excavation and support in Scheme 2

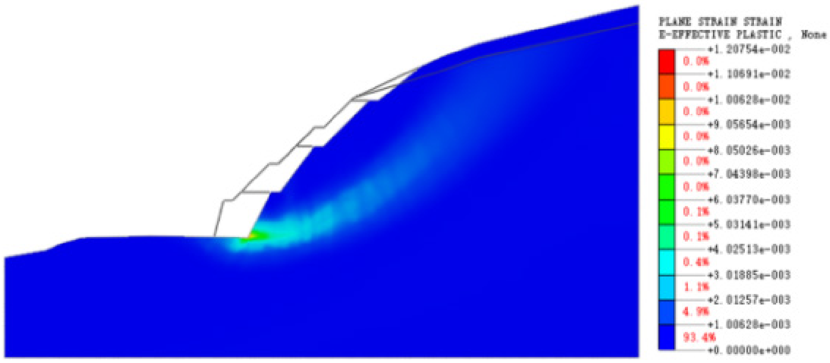


**Figure 11.** The effective plastic nephogram after excavation and support in Scheme 2

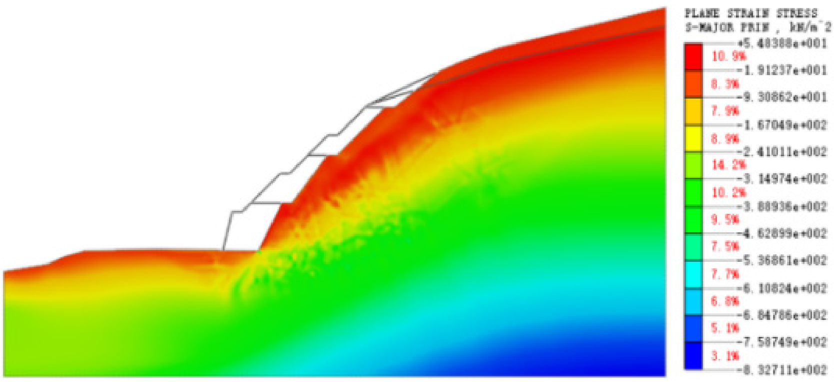


**Figure 12.** The maximum principal stress nephogram after excavation and support in Scheme 2

The two schemes were compared and selected based on factors such as cost, construction period, construction safety, and land acquisition, as shown in **Table 3**.

**Table 3. Comparative analysis of slope widening schemes**

| Evaluation factors | Scheme 1 | Scheme 2 |
|---|---|---|
| **Construction and installation fee (10,000 yuan)** | 1565 | 1379 |
| **Construction period (days)** | 80 | 160 |
| **Construction safety** | The working space is mainly limited to the lower part of the slope and has good controllability. | The excavation slope is high, the construction period is long, and construction safety is difficult to control. |
| **Driving safety** | The working area is small and limited to the lower part of the slope, making it easier to control traffic and the safety of drivers | It is difficult to control the falling of stones from high altitude, which poses certain hidden dangers to existing road traffic safety. |
| **Land acquisition and environmental protection** | Excavation within the slope of the old road will cause little ecological damage. | More land acquisition is needed, which will cause great damage to the ecology and landscape. |

It can be seen from the table that both the excavation methods of Scheme 1 and Scheme 2 can meet the slope safety factor requirements. Although the engineering cost of Scheme 1 is 1.86 million yuan, which is more expensive than the construction and installation cost of Scheme 2, the roadbed fill produced by excavating the slope is a low number. However, the construction period of Scheme 1 is 80 days shorter than Scheme 2 and has more advantages in land acquisition, environmental protection, and safety. After comprehensive comparison, a steep slope with strong support of Scheme 1 is more reasonable, and the stone material needed by the project can be obtained through outsourcing.

## 5. Conclusion

Based on the slope analysis module in the MIDAS GTS software, this article simulates two widening methods of the cutting slope in the K114 + 694–K115 + 162 section of the Yong-tai-wen Expressway, combining the construction period, project cost, construction safety, driving safety, and after comparison and selection of land acquisition and relocation, the following conclusions are reached.

In the case of the slope mentioned in this article, the stability of the slope is mainly controlled by the strength of the rock mass, and cracks or fissure intersections have little impact on the stability of the slope.

The safety factor of the current slope is 1.43, which is in a stable state. When the steep slope foot with slope anchor support scheme is adopted, the safety factor of the slope after excavation is 1.28, which is in an unstable state, so retaining measures are used to improve the safety factor to 1.36 which meets the specification requirements. For the gentle slope with a general slope protection scheme, the safety factor after slope excavation is 1.43, and the safety factor after slope excavation is 1.31, so only general protection for the slope is needed to meet the operational requirements.

After a comprehensive comparative analysis, it is shown that the engineering cost of the steep slope with a strong support solution is 1.86 million yuan, which is more expensive than the construction and installation cost of the gentle slope with a general slope protection solution. However, regarding land acquisition, environmental protection, safety, and other factors, the steep slope with a strong support scheme has more advantages. After comprehensive comparison and selection, the steep slope with a strong support scheme for the reconstruction and expansion of the slope is considered more reasonable and reliable. It is hoped that this study can be a reference for other studies.

## Disclosure statement

The authors declare no conflict of interest.

## References


[1] Chen B, Zhang KN, Zhou B, 2010, Process Stability Analysis and Countermeasures for Swelling Soil Slop Project in Road Reconstruction and Expansion. Mining and Metallurgical Engineering, 30(3): 23–26.

[2] Lin TL, He ZM, Cai J, 2014, Analysis and Comparison of Embankment Widening Schemes in Highway Renovation and Expansion Projects. Mining and Metallurgical Engineering, 34(6): 18–21.

[3] Zhou B, 2011, Study on the Stability Control for the Rebuilding Roadside Slope and its Retaining Measurement, thesis, Central South University.

[4] Chen ZS, Li SL, Hao XT, 2021, Research on Key Points of Safety Protection Technology for High Slope Construction in Expressway Reconstruction and Expansion. Brick, 2021(12): 117–118.

[5] Sun KB, Wang JL, Sun JM, et al., 2019, Reliability Analysis of the Disturbance of Existing Bedding Slope Caused by the Reconstruction and Expansion of Brick Tile Expressway. Highway, 64(07): 8–15.

[6] He XH, 2013, Analysis of Construction Plan for Cutting Slope of Expressway Reconstruction and Expansion Based on FLAC$^{3D}$. Highways and Automotive Applications, 2013(03): 123–126.

[7] Lu W, 2020, Research on Key Issues of Secondary Excavation of Existing Anchored Rock Slope during Reconstruction and Expansion of Highway, thesis, Hunan University of Science and Technology.

[8] Gao WJ, 2017, Stability Analysis of High Rock Slope in Expressway Reconstruction, thesis, Chang'an University.

[9] Feng YH, 2017, Stability Analysis and Engineering Technology Research on Secondary Excavation of Existing High Slope of Widened Expressway, thesis, Chang'an University.

[10] Zhang DW, Li GC, Zhao QY, et al., 2018, Research on Rock Slope Excavation Technology for Expressway Reconstruction and Expansion under the Condition of Ensuring Traffic Safety. Journal of China and Foreign Highway, 38(04): 14–18.

[11] Yao R, 2023, Research on Optimization Design of Roadbed Protection in Expressway Reconstruction and Expansion Project. China Highway, 2023(16): 174–177.

[12] Chen XW, 2019, Analysis of High Slope Protection Technology for Expressway Reconstruction and Expansion Projects, Western China Communications Science and Technology, 2019(11):13–16.

[13] Fan ZY, He W, 2017, Slope Support Scheme and Stability Analysis for Expressway Reconstruction and Expansion. Highways and Automotive Applications, 2017(05): 114–116.

[14] Zheng YR, Zhao SY, 2004, Application of Strength Reduction Fem in Soil and Rock Slope. Chinese Journal of Rock Mechanics and Engineering, 2004(19): 3381–3388.

[15] Jiang X, Qiu YJ, Ling JM, 2008, Comparisons of Strength Reduction Method Software for Slope Stability Analysis. Chinese Journal of Underground Space and Engineering, 4(2): 302–309.



**Publisher's note**

Bio-Byword Scientific Publishing remains neutral with regard to jurisdictional claims in published maps and institutional affiliations.